

# **Engineering tetravalent IgGs with enhanced agglutination potencies for trapping vigorously motile sperm in mucin matrix**

Bhawana Shrestha<sup>a</sup>, Alison Schaefer<sup>b</sup>, Elizabeth C. Chavez<sup>c, 1</sup>, Alexander J. Kopp<sup>d</sup>, Timothy M. Jacobs<sup>e, 2</sup>, Thomas R. Moench<sup>f</sup>, and Samuel K. Lai <sup>a, b, e, f, \*</sup>

<sup>a</sup>Department of Microbiology & Immunology, University of North Carolina at Chapel Hill, Chapel Hill, NC 27599, USA

<sup>b</sup>UNC/NCSU Joint Department of Biomedical Engineering, University of North Carolina at Chapel Hill, Chapel Hill, NC 27599, USA

<sup>c</sup>Department of Biology, University of North Carolina at Chapel Hill, Chapel Hill, NC 27599, USA

<sup>d</sup>Department of Health Policy and Management, University of North Carolina at Chapel Hill, Chapel Hill, NC 27599, USA

<sup>e</sup>Division of Pharmacoengineering and Molecular Pharmaceutics, University of North Carolina at Chapel Hill, Chapel Hill, NC 27599, USA

<sup>f</sup>Mucommune, LLC., Durham, NC 27709, USA

\*Corresponding author:

Samuel K. Lai

Division of Pharmacoengineering and Molecular Pharmaceutics

University of North Carolina at Chapel Hill

Marsico Hall 4213, 125 Mason Farm Road

Chapel Hill, NC 27599

Email: [lai@unc.edu](mailto:lai@unc.edu)

Fax: (+001)-919-843-1232

Homepage: <https://pharmacy.unc.edu/lai-research-group/>

Bhawana Shrestha: [bhawana@email.unc.edu](mailto:bhawana@email.unc.edu)

Alison Schaefer: [amschaef@email.unc.edu](mailto:amschaef@email.unc.edu)

Elizabeth C. Chavez: [ecchavez@bu.edu](mailto:ecchavez@bu.edu)

Alexander J. Kopp: [alexkopp@email.unc.edu](mailto:alexkopp@email.unc.edu)

Timothy M. Jacobs: [timjacobs2@gmail.com](mailto:timjacobs2@gmail.com)

Thomas R. Moench: [thomas.moench@mappbio.com](mailto:thomas.moench@mappbio.com)

---

<sup>1</sup> Department of Microbiology, Boston University, Boston, MA 02118, USA

<sup>2</sup> Dualogics LLC., Durham, NC 27713, USA

## Abstract

Multivalent antibodies such as sIgA can crosslink motile entities such as sperm and bacteria, creating agglomerates that are too large to permeate the dense mucin matrix in mucus, a process commonly referred to as immune exclusion. Unfortunately, sIgA remains challenging to produce in large quantities, and easily aggregates, which prevented their use in clinical applications. To develop sIgA-like tetravalent antibodies that are stable and can be easily produced in large quantities, we designed two IgGs possessing 4 identical Fab domains, with the Fabs arranged either in serial or in the diametrically opposite orientation. As a proof-of-concept, we engineered these tetravalent IgG constructs to bind a ubiquitous sperm antigen using a Fab previously isolated from an immune infertile woman. Both constructs possess at least 4-fold greater agglutination potency and induced much more rapid sperm agglutination than the parent IgG, while exhibiting comparable production yields and identical thermostability as the parent IgG. These tetravalent IgGs offer promise for non-hormonal contraception and underscores the multimerization of IgG as a promising strategy to enhance antibody effector functions based on immune exclusion.

**Keywords: agglutination; antibodies; antibody engineering; contraception; sperm; tetravalent IgG**

## 1. Introduction

More antibodies (Ab) are secreted into mucus than the blood and lymph[1,2], where they are able to work in tandem with mucins to block foreign entities (virus, bacteria, cells) from permeating through the mucus layer and reaching target cells of interest[3,4]. When encountering low concentrations of foreign entities as common with most viral transmissions, the Fc domain of Ab can interact with mucins to facilitate crosslinking of virus-Ab complexes to the mucin mesh, commonly referred to as muco-trapping[3–5]. When encountering high concentrations of foreign entities such as bacteria and sperm, Ab (particularly polyvalent Ab) can also crosslink multiple foreign bodies together into clumps that are either too large to diffuse through mucus, or swim in a coordinated fashion towards target epithelium, a phenomenon commonly referred to as agglutination. Agglutination is particularly effective against motile species as they are much more likely to collide with each other and become agglutinated compared to diffusive species. Agglutination results in not only in an increase in hydrodynamic diameter, but more importantly an effective neutralization of the net forward motion of motile species.

Owing to its prevalence at mucosal surfaces and strong agglutination potency due to the diametrically-opposite orientation of the 4 Fab domains, sIgA represents an attractive format to develop Ab against highly motile species commonly encountered at mucosal surfaces, such as bacteria and sperm[6]. Unfortunately, there has been limited success advancing sIgA for mucosal applications in humans, in part because of manufacturing challenges and stability issues with sIgA and IgM. Recombinant production of sIgA suffer from low production yields and stability due to its complex structure comprising 2 IgA antibodies linked together by the J chain and secretory component[7–9]. Similarly, the lack of scalable purification and homogenous expression remain the main challenges behind recombinant IgM production because of the large size and complexity of IgM structure[10–12]. In contrast, IgGs are highly stable and easy to produce, making IgG the most common Ab format for the development of biologics[13]. We

hypothesized that we could overcome the instability and production challenges of sIgA as well as the limited agglutination potency of IgG by creating IgG molecules with 4 Fabs, identical to sIgA. This includes two different formats: “Fab-IgG” and “IgG-Fab”, based on linking an additional Fab to either the N- or C- terminus respectively, of a parent IgG using a flexible glycine-serine linker (Fig. 1a). We specifically engineered these two formats because IgG-Fab possess structural similarity to sIgA with diametrically opposite Fabs, while Fab-IgG is a commonly studied tetravalent-IgG format[14,15]. The comparison of Fab-IgG and IgG-Fab formats, which differ only in the location of the additional appended Fab fragment, could provide critical insights into the importance of geometric orientation in the agglutination potency of Abs.

As a proof-of-concept to assess agglutination potencies, we engineered the tetravalent and parent IgGs to bind sperm, as a potential approach to enable safe and effective non-hormonal contraception. Globally, over 40% of all pregnancies are unintended, which creates an enormous burden on healthcare systems[16], including over \$20 billion per year in the U.S. alone[17,18]. Despite the availability of cheap and effective contraceptive methods such as progestin and/or estrogen birth control pills and intrauterine devices (IUD), many women are dissatisfied with available contraceptive methods, particularly due to real and/or perceived side-effects associated with the use of exogenous hormones, including increased risks of breast cancer, depression, prolonged menstrual cycle, nausea and migraines[19,20]. Many women are also restricted from using estrogen-based hormonal contraceptives due to medical contraindications[21–23]. Current non-hormonal contraceptives are limited to detergent-based spermicides (e.g. nonoxynol-9), which are toxic to mucosal surfaces and substantially increase the risks of STI transmission, and the copper-IUD, which, though highly effective, is adopted only by a small and declining fraction of women due to heavy menstrual bleeding and its relative invasiveness[24]. These realities strongly underscore the need for convenient non-hormonal contraceptives.

Sperm possess vigorous motility, and women are frequently exposed to a very high concentration of sperm in semen in the vagina. Interestingly, anti-sperm antibodies (ASAs) in infertile women can readily agglutinate and arrest highly motile sperm in mucus, thereby preventing sperm from permeating through mucus and reaching the egg[25,26]. Vaginal delivery of sperm agglutinating ASA exhibited considerable contraceptive efficacy in a rabbit model, reducing embryo formation by 95% in the highly fertile rabbit model[27]. Unfortunately, this approach had not been translated into a clinical setting, due to limited agglutination potencies of IgG. Previous work has shown that CD52g, a glycoform of CD52, is universally present in abundant quantities on the surface of all sperm yet absent in all other tissues and women, establishing CD52g as a highly promising target for contraceptive mAbs [28–30]. Using a Fab domain isolated from an immune infertile but otherwise healthy woman[31,32], we engineered Fab-IgG and IgG-Fab against CD52g, and assessed their agglutination potencies compared to the parent IgG.

## 2. Materials and methods.

### 2.1. Study design and ethics

All studies were performed following a protocol approved by the Institutional Review Board of the University of North Carolina at Chapel Hill (IRB-101817). Informed written consent was obtained from all male and female subjects before the collection of any material.

## 2.2. Cloning and expression of the parent and tetravalent anti-sperm IgG Abs

The variable heavy ( $V_H$ ) and variable light ( $V_L$ ) DNA sequences for anti-sperm IgG1 Ab were obtained from the published sequence of H6-3C4 mAb[31,32]. For light chain (LC) production, a gene fragment consisting of  $V_L$  and  $C_L$  sequences (Integrated DNA Technologies, Coralville, IA) was cloned into an empty mammalian expression vector (pAH, ThermoFisher Scientific) using KpnI (5') and EcoRI (3') restriction sites. For parent IgG and Fab-IgG heavy chain (HC) production,  $V_H$  and  $V_H/C_H1-(G_4S)_6$  linker- $V_H$  gene fragments (GeneArt, ThermoFisher Scientific) were respectively cloned into mammalian IgG1 expression vector comprising of only  $C_H1-C_H2-C_H3$  DNA sequence using KpnI (5') and NheI (3') restriction sites. For IgG-Fab HC production,  $(G_4S)_6$  linker- $V_H/C_H1$  was cloned into the parent IgG expression plasmid using BamHI (5') and MluI (3') restriction sites.

The expression plasmids encoding HC and LC sequences were co-transfected into Expi293F cells using ExpiFectamine™ 293 Transfection reagents (Gibco, Gaithersburg, MD)[33]. For IgG expression, HC and LC plasmid were co-transfected using a 1:1 ratio at 1  $\mu$ g total DNA per 1 mL of culture. For Fab-IgG and IgG-Fab expression, HC and LC plasmid were co-transfected using a 1:2 ratio at 1  $\mu$ g total DNA per 1 mL culture. Transfected Expi293F cells were grown at 37°C in a 5% CO<sub>2</sub> incubator and shaken at 125 r.p.m. for 3-5 days. Supernatants were harvested by centrifugation at 12,800 g for 10 min and passed through 0.22  $\mu$ m filters. Briefly, Abs were purified using standard protein A/G chromatography method. 30 mL of purified supernatants were incubated with 600  $\mu$ L Pierce protein A/G agarose resins (Thermofisher Scientific) overnight at 4°C and loaded into Econo-Pac® Chromatography Columns (Bio-Rad). Resins were washed three times with 1X phosphate-buffered saline (PBS) and proteins were eluted from the resins using 900  $\mu$ L Pierce™ IgG Elution Buffer (Thermofisher Scientific). The eluants were immediately neutralized with 100  $\mu$ L UltraPure™ 1M Tris-HCl, pH 8.0 (Thermofisher Scientific). Next, purified Abs were quantified using absorbance at 280 nm along with the corresponding protein extinction coefficients[34]. The extinction coefficients for IgG, Fab-IgG and IgG-Fab were calculated to be 245400, 415980 and 415980 respectively.

## 2.3. Characterization of the parent and tetravalent anti-sperm IgG Abs

The molecular size of the purified Abs was determined using sodium dodecyl sulfate–polyacrylamide gel electrophoresis (SDS-PAGE) at reducing and non-reducing conditions. For each sample, 1  $\mu$ g of protein was diluted in 3.75  $\mu$ L lithium dodecyl sulfate (LDS) sample buffer followed by the addition of 11.25  $\mu$ L nuclease-free water. Proteins were then denatured at 70°C for 10 min. Next, 0.3  $\mu$ L of 0.5 M tris (2-carboxyethyl) phosphine (TCEP) was added as a reducing agent to the denatured protein for reduced samples and incubated at room temperature for 5 min. Bio-Rad Precision Protein Plus Unstained Standard and Novex™ Sharp Pre-stained Protein Standard were used as ladders. After loading the samples, the gel was run for 50 min at a constant voltage of 200 V. The protein bands were visualized by staining with Imperial Protein Stain (Thermo Scientific) for 1 hr followed by overnight de-staining with Milli-Q water. Image J software (Fiji) was used to adjust the brightness and contrasts of the SDS-PAGE gel for visual purposes.

Size exclusion chromatography with multiple angle light scattering (SEC-MALS) was used to determine the weight average molar weight (MW) and the homogeneity of the purified Abs[35]. The experimental setup consisted of a GE Superdex 200 10/300 column connected to an Agilent

FPLC system, a Wyatt DAWN HELEOS II multi-angle light-scattering instrument, and a Wyatt T-rEX refractometer. Experiments were performed at room temperature with a flow rate maintained at 0.5 mL/min. The column was equilibrated with 1X PBS pH 7.4 containing 200 mg/L of NaN<sub>3</sub> before sample loading. 50-100  $\mu$ L of each sample (1 mg/mL) was injected onto the column, and the MALS data were collected and analyzed using Wyatt ASTRA software (Ver. 6). As the solutes moves through the SEC-MALS system, they scatter light, and the detectors placed at various angles (with respect to the LASER) measure the scattered light intensities at these angles, and the refractometer measures the concentration of the solutes (as refractive index is proportional to the concentration of the solutes) at each time point. Using these values, ASTRA software fits the data to a Debye plot[36,37] and determines the MW of the solutes eluting in different peaks, unequivocally, without using any standards.

The T<sub>m</sub> and T<sub>agg</sub> of the purified Abs were determined using nano differential scanning fluorimetry (nanoDSF; Nanotemper Prometheus NT.48 system)[38]. Samples were diluted to 0.5 mg/mL in 1X PBS at pH 7.4 and loaded into Prometheus NT.48 capillaries. Thermal denaturation experiments were performed from 20°C to 95°C at the rate of 1°C/min, measuring the intrinsic tryptophan fluorescence at 330 nm and 350 nm. The T<sub>m</sub> for each experiment was calculated automatically by Nanotemper PR.Thermcontrol software by plotting the ratiometric measurement of the fluorescent signal against increasing temperature. Next, the T<sub>agg</sub> for each experiment was also calculated automatically by Nanotemper PR.Thermcontrol software via the detection of the back-reflection intensity of a light beam that passes through the sample. As the Ab aggregates, it scatters more light, thus, leading to a reduction of the back-reflected light.

#### **2.4. Collection and processing of semen samples**

Healthy male subjects were asked to refrain from sexual activity for at least 24 hr before semen collection. Semen was collected by masturbation into sterile 50 mL sample cups and incubated for a minimum of 15 min post-ejaculation at room temperature to allow liquefaction. Semen volume was measured, and the density gradient sperm separation procedure (Irvine Scientific, Santa Ana, CA) was used to extract motile sperm from liquefied ejaculates. Briefly, 1.5 mL of liquified semen was carefully layered over 1.5 mL of Isolate® (90% density gradient medium, Irvine Scientific) at room temperature, and centrifuged at 300 g for 20 min. Following centrifugation, the upper layer containing dead cells and seminal plasma was carefully removed without disturbing the motile sperm pellet in the lower layer. The sperm pellet was then washed twice with the sperm washing medium (Irvine Scientific) by centrifugation at 300 g for 10 min. Finally, the purified motile sperm pellet was resuspended in the sperm washing medium, and an aliquot was taken for determination of sperm count and motility using computer-assisted sperm analysis (CASA). All semen samples used in the functional assays exceeded lower reference limits for sperm count ( $15 \times 10^6$  total sperm/mL) and total motility (40%) as indicated by the World Health Organization guidelines[39].

#### **2.5. Sperm count and motility using CASA**

The Hamilton-Thorne computer-assisted sperm analyzer, 12.3 version, was used for the sperm count and motility analysis. This device consists of a phase-contrast microscope (Olympus CX41), a camera, an image digitizer, and a computer with a Hamilton-Thorne Ceros 12.3 software to save and analyze the acquired data. For each analysis, 4.4  $\mu$ L of the semen sample was inserted into MicroTool counting chamber slides (Cytonix, Beltsville, MD) and six

randomly selected microscopic fields, near the center of the slide, were imaged and analyzed for progressively motile and non-progressively motile sperm count. The parameters that were assessed by CASA for motility analysis were as follows: average pathway velocity (VAP), the straight-line velocity (VSL), the curvilinear velocity (VCL), the lateral head amplitude (ALH), the beat cross-frequency (BCF), the straightness (STR) and the linearity (LIN). PM sperm were defined as having a minimum of 25  $\mu\text{m/s}$  VAP and 80% of STR. The complete parameters of the Hamilton-Thorne Ceros 12.3 software are listed in Table S1[40,41].

## **2.6. Whole sperm enzyme-linked immunosorbent assay (ELISA)**

Briefly, half-area polystyrene plates (CLS3690, Corning) were coated with  $2 \times 10^5$  sperm per well in 50  $\mu\text{L}$  of NaHCO<sub>3</sub> buffer (pH 9.6). After overnight incubation at 4°C, the plates were centrifuged at the speed of 300 g for 20 min. The supernatant was discarded, and the plates were air-dried for 1 hr at 45°C. The plates were washed once with 1X PBS. 100  $\mu\text{L}$  of 5% milk was incubated at room temperature for 1 hr to prevent non-specific binding of Abs to the microwells. The serial dilution of mAbs in 1% milk was added to the microwells and incubated overnight at 4°C. Motavizumab, a mAb against the respiratory syncytial virus, was constructed and expressed in the laboratory by accessing the published sequence and used as a negative control for this assay[42]. After primary incubation, the plates were washed three times using 1X PBS. Then, the secondary Ab, goat anti-human IgG F(ab')<sub>2</sub> Ab HRP-conjugated (1:10,000 dilutions in 1% milk, 209-1304, Rockland Inc.) was added to the wells and incubated for 1 hr at room temperature. The washing procedure was repeated and 50  $\mu\text{L}$  of the buffer containing substrate (1-Step Ultra TMB ELISA Substrate, Thermo Scientific) was added to develop the colorimetric reaction for 15 min. The reaction was quenched using 50  $\mu\text{L}$  of 2N H<sub>2</sub>SO<sub>4</sub>, and the absorbance at 450 nm (signal) and 570 nm (background) was measured using SpectraMax M2 Microplate Reader (Molecular Devices). Each experiment was done with samples in triplicates and repeated two times as a measure of assay variability.

## **2.6. Scanning electron microscopy**

Briefly,  $20 \times 10^6$  washed sperm was centrifuged at 300 g for 10 min and the supernatant was discarded without disturbing the sperm pellet. Then, 200  $\mu\text{L}$  of Abs or 1X PBS was added to the sperm pellet, mixed by pipetting and incubated for 5 mins using an end-over-end rotator. Next, 200  $\mu\text{L}$  of 4% paraformaldehyde was added to the Ab-sperm solution and incubated for 10 min using an end-over-end rotator. 50  $\mu\text{L}$  of fixed sperm sample was filtered and washed through membrane filters (10562, K04CP02500, Osmonics, Minnetonka, MN) using 0.15 M sodium phosphate buffer. The samples were then dehydrated in a graded series of alcohol, transferred to a plate with the transitional solvent, hexamethyldisilazane (Electron Microscopy Sciences, Hatfield, PA), and allowed to dry after one exchange. Next, filters were adhered to aluminum stubs with carbon adhesives and samples were sputter-coated with gold-palladium alloy (Au:Pd 60:40 ratio, 91112, Ted Pella Inc., Redding, CA) to a thickness of 3 nm using Cressington Sputter Coater 208 hr. Six random images were acquired for each sample using a Zeiss Supra 25 FESEM with an SE2 Electron detector at 2500X magnification.

## **2.7. Sperm escape assay**

Briefly, 40  $\mu\text{L}$  aliquots of purified sperm ( $10 \times 10^6$  PM sperm/mL) were transferred to individual 0.2 mL polymerase chain reaction (PCR) tubes. Sperm count and motility were performed again on each 40  $\mu\text{L}$  aliquot using CASA. This count serves as the original (untreated) concentration of

sperm for evaluating the agglutination potencies of respective Ab constructs. Following CASA, 30  $\mu$ L of purified sperm was mixed into 0.2 mL PCR tubes containing 30  $\mu$ L of Abs or sperm washing medium control. The tubes were then fixed at 45° angles for 5 min at room temperature. Following this incubation period, 4.4  $\mu$ L was extracted from the top layer of the mixture with minimal perturbation of the tube and transferred to the CASA instrument to quantify the number of PM sperm. The percentage of the PM sperm that escaped agglutination was computed by dividing the sperm count obtained after treatment with Ab constructs by the original untreated sperm count in each respective tube, correcting for the 2-fold dilution with Ab. Each experimental condition was evaluated in duplicates on each semen specimen, and the average from the two experiments was used in the analysis. Data represent 6 independent experiments with at least n=4 unique semen samples. P values were calculated using a one-way analysis of variance (ANOVA) with Dunnett's multiple comparisons test. 6.25  $\mu$ g/mL was selected as the starting concentration for the escape assay because it was the lowest working concentration for IgG. Similarly, the assay was continued until 0.095  $\mu$ g/mL to determine the dose at which tetravalent IgGs fail.

## **2.8. Agglutination kinetics assay**

Briefly, 4.4  $\mu$ L of purified sperm ( $10 \times 10^6$  PM sperm/mL) was added to 4.4  $\mu$ L of Ab constructs in 0.2 mL PCR tubes followed by gentle mixing. Immediately, a timer was started and 4.4  $\mu$ L of the mixture was transferred to chamber slides. The centerfield of the slides was then imaged and analyzed by CASA instrument every 30 s up to 90 s. The reduction in the percentage of PM sperm at each time point was computed by normalizing the PM sperm count obtained after Ab treatment to the PM sperm count obtained after control treatment with the sperm washing medium. Each experimental condition was evaluated in duplicates on each semen specimen, and the average from the two experiments was used in the analysis. Data represent 6 independent experiments with at least n=4 unique semen samples. P values were calculated using a one-way ANOVA with Dunnett's multiple comparisons test. 6.25  $\mu$ g/mL was selected as the starting concentration for the kinetics assay because it was the lowest working concentration for IgG. Similarly, the assay was continued until 0.39  $\mu$ g/mL to determine the dose at which tetravalent IgGs fail.

## **2.9. Fluorescent labeling of sperm**

Purified sperm were fluorescently labeled using Live/Dead Sperm Viability Kit (Invitrogen, ThermoFisher Scientific). SYBR 14 dye, a membrane-permeant nucleic acid stain, stained the live sperm while propidium iodide, a membrane impermeant nucleic acid stain, stained the dead sperm. SYBR14 and propidium iodide dye were added to 1 mL of washed sperm resulting in final SYBR 14 and PI concentration of 200 nM and 12  $\mu$ M respectively and incubated for 10 min at 36 °C. The sperm-dye solution was washed twice using the sperm washing medium to remove unbound fluorophores by centrifuging at 300 g for 10 min. Next, the labeled motile sperm pellet was resuspended in the sperm washing medium, and an aliquot was taken for determination of sperm count and motility using CASA.

## **2.10. Cervicovaginal mucus (CVM) collection and processing**

CVM was collected as previously described[3]. Briefly, undiluted CVM secretions, averaging 0.5 g per sample, were obtained from women of reproductive age, ranging from 20 to 44 years old, by using a self-sampling menstrual collection device (Instead Softcup). Participants inserted

the device into the vagina for at least 30 s, removed it, and placed it into a 50 mL centrifuge tube for collection. Samples were collected at various times throughout the menstrual cycle, and the cycle phase was estimated based on the last menstrual period date normalized to a 28-day cycle. Samples that were non-uniform in color or consistency were discarded. Donors stated they had not used vaginal products nor participated in unprotected intercourse within 3 days before donating. All samples had pH < 4.5.

## 2.11. Multiple particle tracking of fluorescently labeled sperm in CVM

Multiple particle tracking was performed as previously described[3]. Briefly, fresh CVM was diluted three-fold using sperm washing medium to mimic the dilution and neutralization of CVM by alkaline seminal fluid in humans and titrated to pH 6.8-7.1 using small volumes of 3 N NaOH. Next, 4  $\mu$ L of Abs or control (anti-RSV IgG1) was added to 60  $\mu$ L of diluted and pH-adjusted CVM and mixed well in a CultureWell<sup>TM</sup> chamber slide (Invitrogen, ThermoFisher Scientific) followed by mixing of 4  $\mu$ L of 1 x 10<sup>6</sup> fluorescently labeled PM sperm/mL. Chamber slides were incubated for 5 min at room temperature. Then, translational motions of the fluorescently labeled sperm were recorded using an electron-multiplying charge-coupled-device camera (Evolve 512; Photometrics, Tucson, AZ) mounted on an inverted epifluorescence microscope (AxioObserver D1; Zeiss, Thornwood, NY) equipped with an Alpha Plan-Apo 20/0.4 objective, environmental (temperature and CO<sub>2</sub>) control chamber, and light-emitting diode (LED) light source (Lumencor Light Engine DAPI/GFP/543/623/690). 15 videos (512 x 512 pixels, 16-bit image depth) were captured for each Ab condition with MetaMorph imaging software (Molecular Devices, Sunnyvale, CA) at a temporal resolution of 66.7 ms and spatial resolution of 50 nm (nominal pixel resolution, 0.78  $\mu$ m/pixel) for 10 s. Convolutional neural network-based tracking software, which enables fully automated and high fidelity tracking of the motion of entities captured by high resolution video microscopy, was used to determine x, y location of each sperm from each frame of the video. The x,y coordinates over time were then used to calculate quantitative metrics describing sperm motion, such as VAP, VCL, VSL, and STR[43]. Sperm were classified as PM if they exhibited a VAP and VCL of at least 25  $\mu$ m/s and 20  $\mu$ m/s respectively, as well as a VSL to VAP ratio of at least 0.8[16,17]. Data represent 6 independent experiments, each using a unique combination of CVM and semen specimens. P values were calculated using a one-tailed t-test. 25  $\mu$ g/mL was selected as the working concentration for the muco-trapping assay because it was the lowest working concentration for IgG.

## 2.12. Statistical analysis

All analyses were performed using GraphPad Prism 8 software. For multiple group comparisons, P values were calculated using a one-way ANOVA with Dunnett's multiple comparisons tests. The comparison between control- and anti-sperm Ab-treated fluorescent PM sperm was performed using a one-tailed t-test. In all analyses,  $\alpha=0.05$  for statistical significance. All data are presented as the arithmetic mean  $\pm$  standard deviation.

## 3. Results

Upon transient transfection in mammalian (Expi293F) cells, Fab-IgG and IgG-Fab expressed at comparable levels to the parent IgG (Fig. S1). The parent IgG, Fab-IgG and IgG-Fab all exhibited their expected molecular weights of 150 kDa, 250 kDa and 250 kDa, respectively (Fig. 1b and Fig. S2). Surprisingly, while the parent IgG possessed a small fraction of aggregates that

is commonly observed with IgGs in general, the tetravalent IgGs appeared completely homogeneous with no detectable aggregation (Fig. 1c).

We next evaluated the thermostability of the Fab-IgG and IgG-Fab using differential scanning fluorimetry (DSF). Both constructs exhibited exceptional thermal stability, unfolding only at high temperatures of  $T_{m1}$  (midpoint of unfolding of  $C_{H2}$ )  $\geq 71.1^{\circ}\text{C}$  and  $T_{m2}$  (midpoint of unfolding of Fab and  $C_{H3}$ )  $\geq 80^{\circ}\text{C}$ [14,44,45], comparable to those of the parent IgG (Fig. S3). We next confirmed the binding of Fab-IgG and IgG-Fab to their sperm antigen using a whole sperm ELISA assay. Both constructs bound comparably to the human sperm as the parent IgG at 0.1  $\mu\text{g}/\text{mL}$  (Fig. S4).

Species with the greatest active motility are able to most readily penetrate through mucus. Indeed, progressively motile (PM) sperm is the key sperm fraction responsible for fertilization due to their capacity to swim through mucus to reach the egg. We thus assessed the ability of Fab-IgG and IgG-Fab to agglutinate human sperm, using an *in vitro* sperm escape assay that quantified the number of PM sperm that escaped agglutination when treated with the tetravalent IgGs vs the parent IgG as well as sperm washing media control, determined by CASA[40,41]. Upon agglutination in the escape assay, clumps of sperm quickly settle out by gravitation, resulting in reduction of individual PM sperm. The assay was carried out at the final concentration of 5 million PM sperm/mL, reflecting typical amounts of PM sperm in fertile males[39,46]. We found that Fab-IgG and IgG-Fab both exhibited markedly greater sperm agglutination potency than parent IgG. The minimal mAb concentration needed to reduce PM sperm  $>98\%$  was reduced from 6.25  $\mu\text{g}/\text{mL}$  for the parent IgG to 1.56  $\mu\text{g}/\text{mL}$  for both Fab-IgG and IgG-Fab (Fig. 2a). Although both constructs failed to achieve  $>98\%$  agglutination at 0.39  $\mu\text{g}/\text{mL}$ , they were still able to reduce PM sperm by  $>80\%$  (Fig. 2b). In comparison, the parent IgG at 0.39  $\mu\text{g}/\text{mL}$  offered no detectable reduction in PM sperm populations.

For maximum protection, sufficient number of Ab must bind to the target active species before they permeate through mucus. For instance, sperm must be stopped in mucus before they can swim through the cervix and access the uterus for effective contraception[47]. This suggests Abs that could agglutinate sperm more quickly should provide more effective contraception. Thus, we next quantified the sperm-agglutination kinetics of both tetravalent IgG constructs using CASA, specifically measuring the fraction of agglutinated and free PM sperm over time immediately after mixing washed sperm with different mAbs. At 6.25  $\mu\text{g}/\text{mL}$ , the parent IgG reduced PM sperm by  $\geq 90\%$  within 90s in 5 of 6 semen samples; at 1.56  $\mu\text{g}/\text{mL}$ , the parent IgG failed to do so in all 6 of 6 samples (Fig. 2c). In contrast, Fab-IgG and IgG-Fab achieved  $\geq 90\%$  agglutination within 30s in all 6 of 6 samples at 6.25  $\mu\text{g}/\text{mL}$ , and within 60s in 5 of 6 samples at 1.56  $\mu\text{g}/\text{mL}$ . Notably, the agglutination kinetics of Fab-IgG and IgG-Fab were both markedly faster and more complete than the parent IgG at each Ab concentrations tested and across all timepoints (Fig. 2d). We visually confirmed sperm agglutination by the parent IgG vs. tetravalent IgGs at their effective concentrations using scanning electron microscopy (Fig. 3).

Earlier works have shown that IgA and IgG Abs can completely immobilize individual spermatozoa in the mucus by crosslinking antibody-bound spermatozoa to mucins; this is commonly referred to as the “shaking phenomenon”[26]. We have previously shown that multiple Fc present on Herpes-bound IgGs can effectively immobilize virus in CVM and blocked

vaginal Herpes transmission in mice[3]. Since the Fc region was conserved and identical in both tetravalent IgGs and parent IgG, we hypothesized that Fab-IgG and IgG-Fab constructs will trap individual spermatozoa in mucus similar to native IgG. We used multiple particle tracking to analyze the motion of fluorescently labeled sperm in CVM treated with either control, parent IgG or tetravalent IgGs[43]. Both IgG-Fab and Fab-IgG reduced the fraction of PM sperm to a comparable extent as the parent IgG (Movie S1-S4; Fig. 4), indicating that Fc-mediated crosslinking remained unaffected by the addition of Fabs at both N- and C-terminus.

#### 4. Discussion

Our finding that both tetravalent sperm-binding IgGs, regardless of the orientation of additional Fab domains, effectively agglutinate sperm at a markedly lower concentration than IgG underscores multimerization as the promising strategy for the development of non-hormonal contraceptives. Many of the current multivalent Abs are bispecific or trispecific in nature and must content with potential mispairing of light and heavy chains. As a result, many such engineered Ab formats, such as single-chain variable fragment (scFv) or camel-derived nanobodies, involve a substantial deviation from natural human Ab structure based on the non-covalent pairing of heavy and light chains. scFv-based multivalent Ab constructs frequently suffer from low stability, heterogeneous expression, and decreased affinity and specificity stemming from the removal of the  $C_{H1}/C_L$  interface present in a full-length Fab. The introduction of orthogonal mutations to facilitate heavy and light chain pairing can also substantially reduce mAb yield or overall stability. These limitations do not apply when generating monospecific multivalent IgGs like our tetravalent IgGs, which possess identical and full-length human Fabs. Our strategy to covalently link additional Fabs to a parent heavy chain also contrasts from current multimerization strategies based on self-assembly of multiple IgGs based on Fc-mutations[48] or appending an IgM tail-piece, which often suffers poor homogeneity and stability[49,50]. The combination of fully intact human Fabs and covalent linkages likely contributes to the surprising thermal stability, homogeneity and bioprocessing ease of the tetravalent IgGs developed here. We believe the sperm-agglutinating potency of the tetravalent IgGs could be further enhanced by increasing the number of Fab domains up to 10 Fab per molecule, similar to a potent agglutinator IgM, resulting in extremely potent contraceptive mAbs.

Poor sperm motility in mid-cycle cervical mucus and low total sperm count are both strong correlates to low conception rate. Human semen averages ~45-65 million sperm per mL, 15 million sperm per mL marks the lowest 5<sup>th</sup> percentile in men with proven fertility, and <5 million sperm per mL is considered severe oligospermia with very low fertility[39,46,51]. Additionally, even under ideal circumstances (unprotected intercourse on the cycle day of maximum fertility), the odds of conceiving are low, only ~10%[52]. These finding, together with contraceptive success with topical ASA against rabbit sperm[27], suggest substantial reduction (even if incomplete, e.g.~98%) of progressive sperm motility in the vagina/cervix by contraceptive mAbs should provide highly effective contraception by limiting the number of fertile motile sperm to reach the egg.

Unlike small molecule contraceptives, contraceptive mAbs should be exceptionally safe due to the specificity of targeting, particularly when binding to unique epitopes present only on sperm and not on expressed in female tissues. Safety is likely to be further enhanced by topical

delivery: mAb delivered to mucosal surfaces such as the vagina is poorly absorbed into the systemic circulation[53], and the vagina represents a poor immunization inductive site, with limited immune response even when vaccinating with the aid of highly immunostimulatory adjuvants[54]. Topical delivery also substantially reduces the overall mAb dose needed. Given the limited volume of secretions in the female reproductive tract (FRT), typically  $\leq 1$  mL in the vagina[55], a relatively high concentration of mAb locally can be achieved even with very limited total quantities of mAb dosed. In contrast, systemically dosed mAbs must contend with the large blood volume ( $\sim 5$ L), distribution to non-target tissues, natural catabolic degradation, and limited distribution into the FRT. The reduced quantities of mAb needed to sustain contraceptive levels in the FRT with vaginal delivery should translate to substantially lower amounts of total mAb needed, and consequently, cost savings.

Given the abundance of endogenous IgGs in the vagina and long half-life of vaginally instilled IgG i.e.  $\sim 9$  hrs[56,57], locally delivered contraceptive mAbs should remain extremely stable and active in the FRT. Contraceptive mAbs can be delivered using multiple methods. For instance, to enable rapid and transient contraception, mAbs can be formulated into quick-dissolving vaginal film to provide on-demand non-hormonal contraception, effective over a 12-24 hrs period. In addition, contraceptive mAbs can be released from intravaginal rings (IVRs), enable month-long contraception comparable to the Nuvaring®. The ability to stably release antibodies from IVRs was recently demonstrated in rhesus macaques[58].

### **Statement of significance**

Currently, there are limited methods to reinforce the mucus gel barrier against species with active motility. Here, we demonstrate that we can greatly enhance the agglutination potencies through carefully engineering tetrameric antibody, which induces the formation of agglutinates too large to permeate mucus. As a proof-of-concept, we engineered tetravalent anti-sperm antibodies that can effectively agglutinate human sperm and trap sperm in human mucus. Our work paves the way of developing potent multivalent antibodies for non-hormonal contraception, which may address the contraceptive needs of millions of women who risk unintended pregnancies, due to medical contraindications and/or perceived or real side-effects associated with the use of hormonal contraceptives. Our work not only represents the first contraceptive antibodies with enhanced agglutination potential, but also provides a strategy for reinforcing the mucus barrier against other species with active motility.

### **Author contributions**

B.S. and S.K.L. conceptualized the study. B.S. and S.K.L. designed experiments and wrote the manuscript. T.R.M. provided critical feedback and edited the manuscript. B.S., T.M.J. and A.S. engineered and assembled the DNA constructs for Abs. B.S. planned and carried out the expression, purification, and characterization of the Abs. B.S., E.C.C. and A.J.K. planned and performed sperm escape and agglutination kinetics assays. B.S planned and carried out scanning electron microscopy studies and sperm trapping assay. A.S developed an algorithm and analyzed the sperm trapping data.

### **Acknowledgments**

Special thanks to Dr. Deborah O'Brien for providing the CASA instrument and assistance in setting up the CASA measurements. Special thanks to the UNC Macromolecular Interactions

Facility for instruments used in SEC-MALS and DSF studies, and Microscopy Services Laboratory for instruments used in scanning electron microscopy experiments. This work was financially supported by the Eshelman Institute for Innovation (S.K.L.); The David and Lucile Packard Foundation (2013-39274; S.K.L.); National Institutes of Health under grants R56HD095629 (S.K.L.), U54HD096957 (T.R.M. and S.K.L.), R43HD094454 (T.R.M.) and R44HD097063 (T.R.M.); National Science Foundation (DMR-1810168; S.K.L.); and PhRMA Foundation Graduate Fellowship (B.S.).

## Disclosures

S.K.L. is the founder of Mucommune, LLC and currently serves as its interim CEO. S.K.L. is also the founder of Inhalon Biopharma, Inc, and currently serves as its CSO, Board of Directors, and Scientific Advisory Board. S.K.L. has equity interests in both Mucommune and Inhalon Biopharma; S.K.L.’s relationships with Mucommune and Inhalon are subject to certain restrictions under University policy. The terms of these arrangements are managed by UNC-CH in accordance with its conflict of interest policies. T.R.M. has equity interests in Inhalon Biopharma. B.S., A.S., T.M.J., T.R.M., and S.K.L. are inventors on patents licensed by Mucommune and Inhalon Biopharma.

## Data and materials availability

All data and materials are available from the corresponding author upon reasonable request.

## Code availability

The code used to analyze fluorescent PM sperm in vaginal mucus samples is available from the corresponding author upon reasonable request.

## References

- [1] A.J. MacPherson, K.D. McCoy, F.E. Johansen, P. Brandtzaeg, The immune geography of IgA induction and function, *Mucosal Immunol.* 1 (2008) 11–22. <https://doi.org/10.1038/mi.2007.6>.
- [2] N.J. Mantis, N. Rol, B. Corthésy, Secretory IgA’s complex roles in immunity and mucosal homeostasis in the gut, *Mucosal Immunol.* 4 (2011) 603–611. <https://doi.org/10.1038/mi.2011.41>.
- [3] Y.Y. Wang, A. Kannan, K.L. Nunn, M.A. Murphy, D.B. Subramani, T. Moench, R. Cone, S.K. Lai, IgG in cervicovaginal mucus traps HSV and prevents vaginal Herpes infections, *Mucosal Immunol.* 7 (2014) 1036–1044. <https://doi.org/10.1038/mi.2013.120>.
- [4] Y.Y. Wang, D. Harit, D.B. Subramani, H. Arora, P.A. Kumar, S.K. Lai, Influenza-binding antibodies immobilise influenza viruses in fresh human airway mucus, *Eur Res J.* 49 (2017) 1–4. <https://doi.org/10.1183/13993003.01709-2016>.
- [5] C.E. Henry, Y.Y. Wang, Q. Yang, T. Hoang, S. Chattopadhyay, T. Hoen, L.M. Ensign, K.L. Nunn, H. Schroeder, J. McCallen, T. Moench, R. Cone, S.R. Roffler, S.K. Lai, Anti-PEG antibodies alter the mobility and biodistribution of densely PEGylated nanoparticles in mucus, *Acta Biomater.* 43 (2016) 61–70. <https://doi.org/10.1016/j.actbio.2016.07.019>.
- [6] J.M. Woof, M.A. Kerr, The function of immunoglobulin A in immunity, *J. Pathol.* 208 (2006) 270–282. <https://doi.org/10.1002/path.1877>.
- [7] M. Paul, R. Reljic, K. Klein, P.M.W. Drake, C. Van Dolleweerd, M. Pabst, M. Windwarder, E. Arcalis, E. Stoger, F. Altmann, C. Cosgrove, A. Bartolf, S. Baden, J.K.

Ma, Characterization of a plant-produced recombinant human secretory IgA with broad neutralizing activity against HIV, *MAbs*. 6 (2014) 1585–1597.

[8] V. Virdi, P. Juarez, V. Boudolf, A. Depicker, Recombinant IgA production for mucosal passive immunization, advancing beyond the hurdles, *Cell. Mol. Life Sci.* 73 (2016) 535–545. <https://doi.org/10.1007/s00018-015-2074-0>.

[9] K.T. Barnhart, M.J. Rosenberg, H.T. MacKay, D.L. Blithe, J. Higgins, T. Walsh, L. Wan, M. Thomas, M.D. Creinin, C. Westhoff, W. Schlaff, D.F. Archer, C. Ayers, A. Kaunitz, S. Das, T.R. Moench, Contraceptive efficacy of a novel spermicidal microbicide used with a diaphragm: A randomized controlled trial, *Obstet. Gynecol.* 110 (2007) 577–586. <https://doi.org/10.1097/01.AOG.0000278078.45640.13>.

[10] A. Mader, V. Chromikova, R. Kunert, Recombinant IgM expression in mammalian cells: A target protein challenging biotechnological production, *Adv. Biosci. Biotechnol.* 04 (2013) 38–43. <https://doi.org/10.4236/abb.2013.44a006>.

[11] V. Chromikova, A. Mader, W. Steinfellner, R. Kunert, Evaluating the bottlenecks of recombinant IgM production in mammalian cells, *Cytotechnology*. 67 (2015) 343–356. <https://doi.org/10.1007/s10616-014-9693-4>.

[12] Y. Azuma, Y. Ishikawa, S. Kawai, T. Tsunenari, H. Tsunoda, T. Igawa, S.I. Iida, M. Nanami, M. Suzuki, R.F. Irie, M. Tsuchiya, H. Yamada-Okabe, Recombinant human hexamer-dominant IgM monoclonal antibody to ganglioside GM3 for treatment of melanoma, *Clin. Cancer Res.* 13 (2007) 2745–2750. <https://doi.org/10.1158/1078-0432.CCR-06-2919>.

[13] A.L. Nelson, E. Dhimolea, J.M. Reichert, Development trends for human monoclonal antibody therapeutics, *Nat. Rev. Drug Discov.* 9 (2010) 767–774. <https://doi.org/10.1038/nrd3229>.

[14] X. Wu, A.J. Sereno, F. Huang, S.M. Lewis, R.L. Lieu, C. Weldon, C. Torres, C. Fine, M.A. Batt, J.R. Fitchett, A.L. Glasebrook, B. Kuhlman, S.J. Demarest, Fab-based bispecific antibody formats with robust biophysical properties and biological activity, *MAbs*. 7 (2015) 470–482. <https://doi.org/10.1080/19420862.2015.1022694>.

[15] J.T. Huckaby, C.L. Parker, T.M. Jacobs, A. Schaefer, D. Wadsworth, A. Nguyen, A. Wang, J. Newby, S.K. Lai, Engineering Polymer-Binding Bispecific Antibodies for Enhanced Pretargeted Delivery of Nanoparticles to Mucus-Covered Epithelium, *Angew. Chemie - Int. Ed.* 58 (2019) 5604–5608. <https://doi.org/10.1002/anie.201814665>.

[16] J. Bearak, A. Popinchalk, L. Alkema, G. Sedgh, Global, regional, and subregional trends in unintended pregnancy and its outcomes from 1990 to 2014: estimates from a Bayesian hierarchical model Jonathan, *Lancet Glob Heal.* 6 (2018) 380–389. <https://doi.org/10.1016/j.physbeh.2017.03.040>.

[17] L.B. Finer, S.K. Henshaw, Disparities in Rates of Unintended Pregnancy In the United States, 1994 and 2001, *Perspect. Sex. Reprod. Health.* 38 (2006) 90–96. <https://doi.org/10.1363/3809006>.

[18] L.B. Finer, M.R. Zolna, Declines in Unintended Pregnancy in the United States, 2008–2011, *N. Engl. J. Med.* 374 (2016) 843–852. <https://doi.org/10.1056/NEJMsa1506575>.

[19] S.O. Skouby, Contraceptive use and behavior in the 21st century: A comprehensive study across five European countries, *Eur. J. Contracept. Reprod. Heal. Care.* 9 (2004) 57–68. <https://doi.org/10.1080/13625180410001715681>.

[20] J. Brynhildsen, Combined hormonal contraceptives : prescribing patterns , compliance , and benefits versus risks, *Ther. Adv. Drug Saf.* 5 (2014) 201–213.

https://doi.org/10.1177/2042098614548857.

[21] W.W. Beck, Complications and Contraindications of Oral Contraception, *Clin. Obstet. Gynecol.* 24 (1981) 893–902. <https://doi.org/10.1097/00003081-198109000-00016>.

[22] D. Grossman, K. White, K. Hopkins, J. Amastae, M. Shedlin, J.E. Potter, Contraindications to combined oral contraceptives among over-the-counter compared with prescription users, *Obstet. Gynecol.* 117 (2011) 558–565. <https://doi.org/10.1097/AOG.0b013e31820b0244>.

[23] J.W. Roos-Hesselink, J. Cornette, K. Sliwa, P.G. Pieper, G.R. Veldtman, M.R. Johnson, Contraception and cardiovascular disease, *Eur. Heart J.* 36 (2015) 1728–1734. <https://doi.org/10.1093/eurheartj/ehv141>.

[24] K. Daniels, J. Daugherty, J. Jones, W. Mosher, Current Contraceptive Use and Variation by Selected Characteristics Among Women Aged 15–44: United States, 2011–2013, *Natl. Cent. Heal. Stat.* (2015) 1014–1018.

[25] J. Kremer, S. Jager, The Sperm-Cervical Mucus Contact Test: A Preliminary Report, *Fertil. Steril.* 27 (1976) 335–340. [https://doi.org/10.1016/S0015-0282\(16\)41726-7](https://doi.org/10.1016/S0015-0282(16)41726-7).

[26] G.N. Clarke, Induction of the Shaking Phenomenon by IgA Class Antispermatozoal Antibodies From Serum, *Am. J. Reprod. Immunol. Microbiol.* 9 (1985) 12–14. <https://doi.org/10.1111/j.1600-0897.1985.tb00333.x>.

[27] P.E. Castle, K.J. Whaley, T.E. Hoen, T.R. Moench, R.A. Cone, Contraceptive Effect of Sperm-Agglutinating Monoclonal Antibodies in Rabbits, *Biol. Reprod.* 56 (1997) 153–159. <https://doi.org/10.1095/biolreprod56.1.153>.

[28] A.B. Diekman, E.J. Norton, K.L. Klotz, V.A. Westbrook, H. Shibahara, S. Naaby-Hansen, C.J. Flickinger, J.C. Herr, N-linked glycan of a sperm CD52 glycoform associated with human infertility, *FASEB J.* 13 (1999) 1303–1313. <https://doi.org/10.1096/fasebj.13.11.1303>.

[29] E.J. Norton, A.B. Diekman, V.A. Westbrook, D.W. Mullins, K.L. Klotz, L.L. Gilmer, T.S. Thomas, D.C. Wright, J. Brisker, V.H. Engelhard, C.J. Flickinger, J.C. Herr, A male genital tract-specific carbohydrate epitope on human CD52: Implications for immunocontraception, *Tissue Antigens.* 60 (2002) 354–364. <https://doi.org/10.1034/j.1399-0039.2002.600502.x>.

[30] D.J. Anderson, P.M. Johnson, N.J. Alexander, W.R. Jones, P.D. Griffin, Monoclonal antibodies to human trophoblast and sperm antigens: Report of two WHO-sponsored workshops, June 30, 1986-Toronto, Canada, *J. Reprod. Immunol.* 10 (1987) 231–257. [https://doi.org/10.1016/0165-0378\(87\)90089-1](https://doi.org/10.1016/0165-0378(87)90089-1).

[31] S. Isojima, K. Kameda, Y. Tsuji, M. Shigeta, Y. Ikeda, K. Koyama, Establishment and characterization of a human hybridoma secreting monoclonal antibody with high titers of sperm immobilizing and agglutinating activities against human seminal plasma, *J. Reprod. Immunol.* 10 (1987) 67–78. [https://doi.org/10.1016/0165-0378\(87\)90051-9](https://doi.org/10.1016/0165-0378(87)90051-9).

[32] S. Komori, N. Yamasaki, M. Shigeta, S. Isojima, T. Watanabe, Production of heavy-chain class-switch variants of human monoclonal antibody by recombinant DNA technology, *Clin. Exp. Immunol.* 71 (1988) 508–516. [https://doi.org/10.1007/978-3-211-89836-9\\_877](https://doi.org/10.1007/978-3-211-89836-9_877).

[33] R. Vazquez-Lombardi, D. Nevoltris, A. Luthra, P. Schofield, C. Zimmermann, D. Christ, Transient expression of human antibodies in mammalian cells, *Nat. Protoc.* 13 (2018) 99–117. <https://doi.org/10.1038/nprot.2017.126>.

[34] G.Y. Wiederschain, The proteomics protocols handbook, *Biochem.* 71 (2006) 696–696. <https://doi.org/10.1134/s0006297906060150>.

[35] D. Some, H. Amartely, A. Tsadok, M. Lebendiker, Characterization of proteins by size-exclusion chromatography coupled to multi-angle light scattering (Sec-mals), *J. Vis. Exp.* 2019 (2019) 1–9. <https://doi.org/10.3791/59615>.

[36] P. Debye, Light scattering in solutions, *J. Appl. Phys.* 15 (1944). <https://doi.org/10.1088/0150-536X/25/1/002>.

[37] M. Andersson, B. Wittgren, K.G. Wahlund, Accuracy in multiangle light scattering measurements for molar mass and radius estimations. Model calculations and experiments, *Anal. Chem.* 75 (2003) 4279–4291. <https://doi.org/10.1021/ac030128+>.

[38] A. Real-Hohn, M. Groznica, N. Löffler, D. Blaas, H. Kowalski, nanoDSF: In vitro Label-Free Method to Monitor Picornavirus Uncoating and Test Compounds Affecting Particle Stability, *Front. Microbiol.* 11 (2020) 1–12. <https://doi.org/10.3389/fmicb.2020.01442>.

[39] W.H. Organization, Examination and processing of human semen, in: World Health, 2010: pp. 1–271. <https://doi.org/10.1038/aja.2008.57>.

[40] Y. Hirano, H. Shibahara, H. Obara, T. Suzuki, S. Takamizawa, C. Yamaguchi, H. Tsunoda, I. Sato, Relationships between sperm motility characteristics assessed by the computer-aided sperm analysis (CASA) and fertilization rates in vitro, *J. Assist. Reprod. Genet.* 18 (2001) 213–218. <https://doi.org/10.1023/A:1009420432234>.

[41] A. Mitra, R.T. Richardson, M.G. O’Rand, Analysis of Recombinant Human Semenogelin as an Inhibitor of Human Sperm Motility, *Biol. Reprod.* 82 (2010) 489–496. <https://doi.org/10.1095/biolreprod.109.081331>.

[42] H. Wu, D.S. Pfarr, S. Johnson, Y.A. Brewah, R.M. Woods, N.K. Patel, W.I. White, J.F. Young, P.A. Kiener, Development of Motavizumab, an Ultra-potent Antibody for the Prevention of Respiratory Syncytial Virus Infection in the Upper and Lower Respiratory Tract, *J. Mol. Biol.* 368 (2007) 652–665. <https://doi.org/10.1016/j.jmb.2007.02.024>.

[43] J.M. Newby, A.M. Schaefer, P.T. Lee, M.G. Forest, S.K. Lai, Convolutional neural networks automate detection for tracking of submicron-scale particles in 2D and 3D, *Proc. Natl. Acad. Sci. U. S. A.* 115 (2018) 9026–9031. <https://doi.org/10.1073/pnas.1804420115>.

[44] E. Garber, S.J. Demarest, A broad range of Fab stabilities within a host of therapeutic IgGs, *Biochem. Biophys. Res. Commun.* 355 (2007) 751–757. <https://doi.org/10.1016/j.bbrc.2007.02.042>.

[45] R.M. Ionescu, J. Vlasak, C. Price, M. Kirchmeier, Contribution of Variable Domains to the Stability of Humanized IgG1 Monoclonal Antibodies, *J. Pharm. Sci.* 97 (2008) 1414–1426. <https://doi.org/10.1002/jps>.

[46] R.M. Sharpe, Sperm counts and fertility in men: A rocky road ahead. *Science & Society Series on Sex and Science*, *EMBO Rep.* 13 (2012) 398–403. <https://doi.org/10.1038/embor.2012.50>.

[47] D.S. Fordney Settlage, M. Motoshima, D.R. Tredway, Sperm Transport from the External Cervical Os to the Fallopian Tubes in Women: A Time and Quantitation Study, *Fertil. Steril.* 24 (1973) 655–661. [https://doi.org/10.1016/s0015-0282\(16\)39908-3](https://doi.org/10.1016/s0015-0282(16)39908-3).

[48] C.A. Diebold, F.J. Beurskens, R.N. De Jong, R.I. Koning, K. Strumane, M.A. Lindorfer, M. Voorhorst, D. Ugurlar, S. Rosati, A.J.R. Heck, J.G.J. Van De Winkel, I.A. Wilson, A.J. Koster, R.P. Taylor, E.O. Saphire, D.R. Burton, J. Schuurman, P. Gros, P.W.H.I. Parren, Complement is activated by IgG hexamers assembled at the cell surface, *Science* (80-. ). 343 (2014) 1260–1263. <https://doi.org/10.1126/science.1248943>.

[49] V. Sorensen, V. Sundvold, T.E. Michaelsen, I. Sandlie, Polymerization of IgA and IgM:

roles of Cys309/Cys414 and the secretory tailpiece., *J. Immunol.* 162 (1999) 3448–55.  
<http://www.ncbi.nlm.nih.gov/pubmed/10092800>.

[50] K. Teye, K. Hashimoto, S. Numata, K. Ohta, M. Haftek, T. Hashimoto, Multimerization is required for antigen binding activity of an engineered IgM/IgG chimeric antibody recognizing a skin-related antigen, *Sci. Rep.* 7 (2017) 1–12.  
<https://doi.org/10.1038/s41598-017-08294-2>.

[51] A. Hirsh, Male subfertility, *Br. Med. J.* 327 (2003) 669–672.  
<https://doi.org/https://doi.org/10.1136/bmj.327.7416.669>.

[52] D. Li, A.J. Wilcox, D.B. Dunson, Benchmark Pregnancy Rates and the Assessment of Post-coital Contraceptives: An Update, *Contraception.* 91 (2015) 344–349.  
<https://doi.org/10.1016/j.physbeh.2017.03.040>.

[53] A. Hussain, F. Ahsan, The vagina as a route for systemic drug delivery, *J. Control. Release.* 103 (2005) 301–313. <https://doi.org/10.1016/j.jconrel.2004.11.034>.

[54] L. Zeitlin, R.A. Cone, K.J. Whaley, Using Monoclonal Antibodies to Prevent Mucosal Transmission of Epidemic Infectious Diseases., *Emerg. Infect. Dis.* 5 (1999) 54–64.

[55] D.H. Owen, D.F. Katz, A vaginal fluid simulant, *Contraception.* 59 (1999) 91–95.  
[https://doi.org/10.1016/S0010-7824\(99\)00010-4](https://doi.org/10.1016/S0010-7824(99)00010-4).

[56] M. Johansson, N.Y. Lycke, Immunology of the human genital tract, *Curr. Opin. Infect. Dis.* 16 (2003) 43–49. <https://doi.org/10.1097/00001432-200302000-00008>.

[57] T. Moench, P. Blumenthal, K. Whaley, Antibodies may provide prolonged microbicidal activity due to their long residence time in the vagina, *Microbicides.* Washington (2000) Abstract B15.

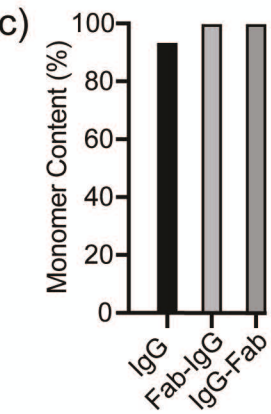
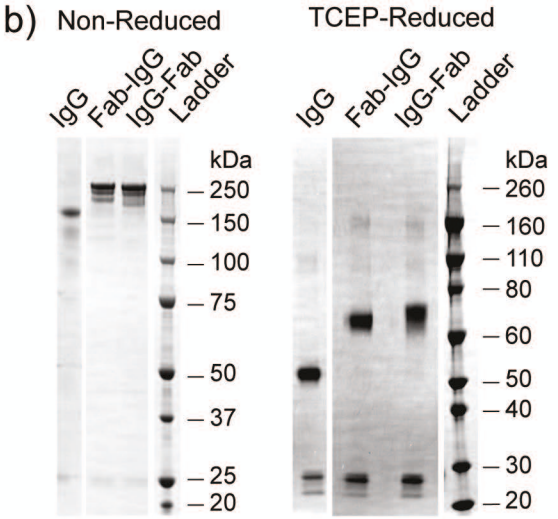
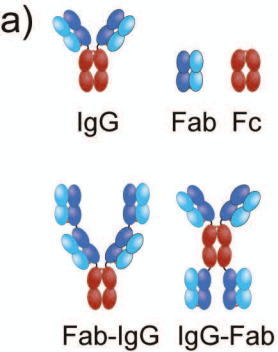
[58] C. Zhao, M. Gunawardana, F. Villinger, M.M. Baum, M. Remedios-Chan, T.R. Moench, L. Zeitlin, K.J. Whaley, O. Bohorov, T.J. Smith, D.J. Anderson, J.A. Moss, Pharmacokinetics and preliminary safety of pod-intravaginal rings delivering the monoclonal antibody VRC01-N for HIV prophylaxis in a macaque model, *Antimicrob. Agents Chemother.* 61 (2017) 1–16. <https://doi.org/10.1128/AAC.02465-16>.

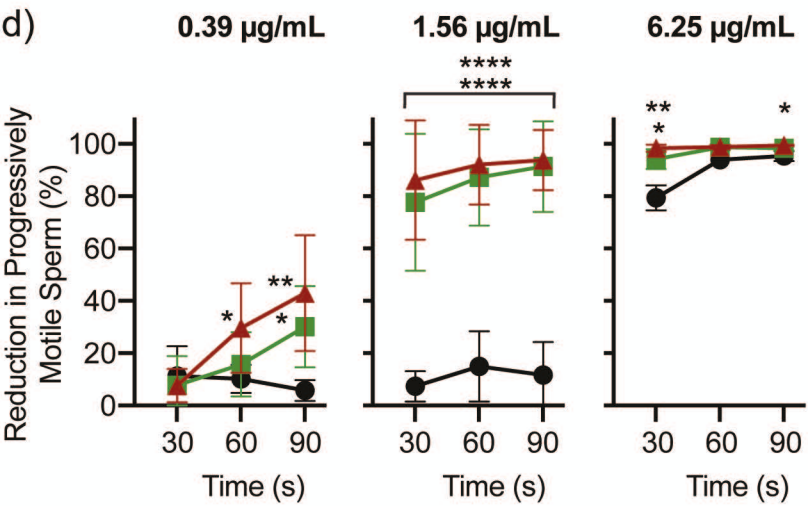
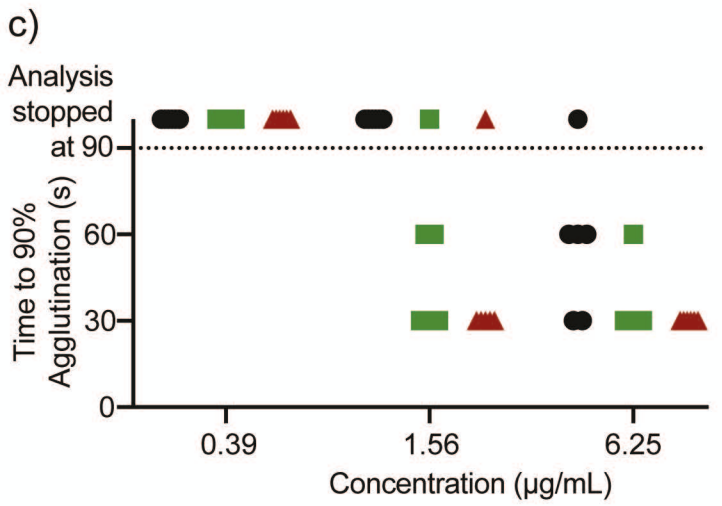
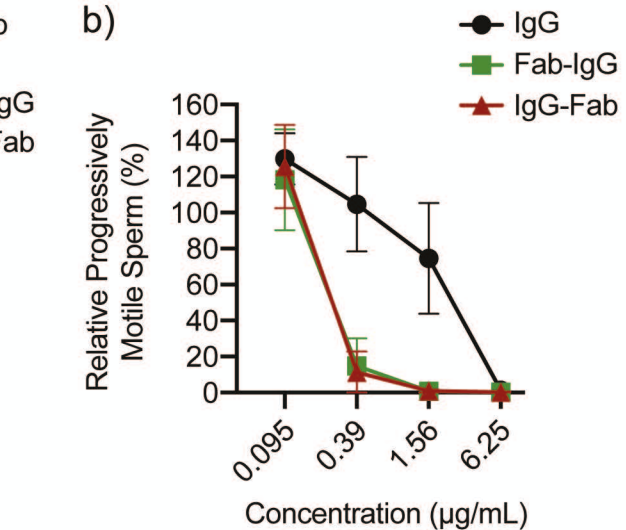
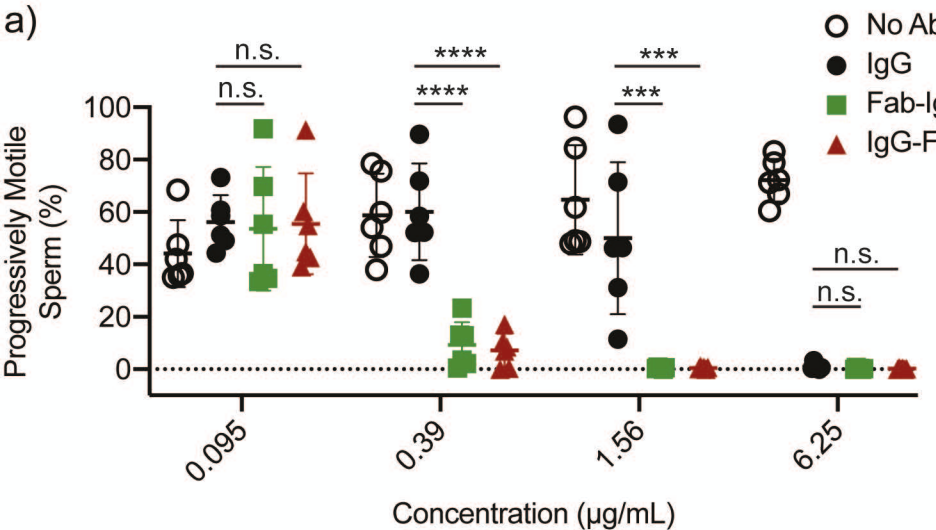
**Fig. 1. Production and characterization of tetravalent anti-sperm IgG Abs.** (a) Schematic diagrams of anti-sperm IgG, Fab-IgG and IgG-Fab. (b) Non-reducing and reducing SDS-PAGE analysis of the indicated Abs (1 µg). (c) Demonstration of the purity and homogeneity of the indicated Abs (50-100 µg) using SEC-MALS analysis. Y-axis indicates the total percentage of Abs representing their theoretical molecular weights.

**Fig. 2. Multimerization markedly enhances the agglutination potency and kinetics of anti-sperm IgG Abs.** (a) Sperm agglutination potency of the parent IgG, Fab-IgG and IgG-Fab measured by the CASA-based quantification of the percentage of sperm that remains PM after Ab-treatment compared to pre-treatment condition. (b) The sperm agglutination potency of the Abs normalized to media control. (c) The sperm agglutination kinetics of the indicated Abs measured by the quantification of time required to achieve 90% agglutination of PM sperm compared to the media control. (d) The rate of sperm agglutination determined by the reduction in the percentage of PM sperm count at three timepoints after Ab-treatment compared to the media control. Purified sperm at the final concentration of  $5 \times 10^6$  PM sperm/mL was used for both agglutination potency and kinetics studies. \*P < 0.05, \*\*P < 0.01, \*\*\*P < 0.001 and \*\*\*\*P < 0.0001. Lines indicate arithmetic mean values and standard deviation.

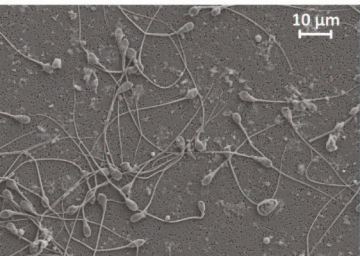
**Fig. 3. Scanning electron microscopy images of the agglutinated sperm.** 20 million washed sperm were treated with IgG, Fab-IgG and IgG-Fab for 5 min and fixed using 4% paraformaldehyde. Images were obtained at 2500X magnification. Scale bar, 10 µm.

**Fig. 4. Tetravalent sperm-binding IgG constructs conserve the trapping potency of the parent IgG.** The trapping potency of the indicated Abs measured by quantifying the percentage of fluorescently labeled PM sperm in Ab-treated CVM using neural network tracker analysis software. 25 µg/mL of Abs and purified sperm at the final concentration of  $5.8 \times 10^4$  PM sperm/mL were used. Motavizumab (anti-RSV IgG) was used as the isotype control. Data were obtained from n = 6 independent experiments with 6 unique combinations of semen and CVM specimens. P values were calculated using a one-tailed t-test between control Ab- and anti-sperm Ab-treated sperm samples. \*P < 0.05. Lines indicate arithmetic mean values and standard deviation.

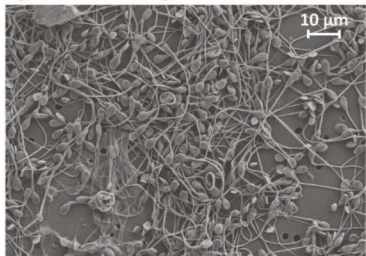




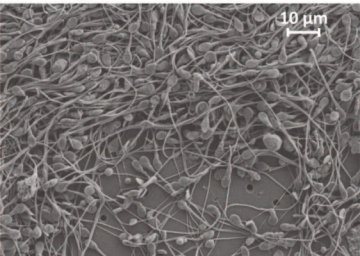
PBS



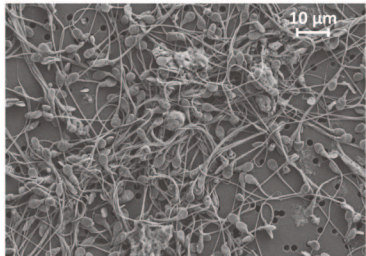
IgG-6.25 μg/mL

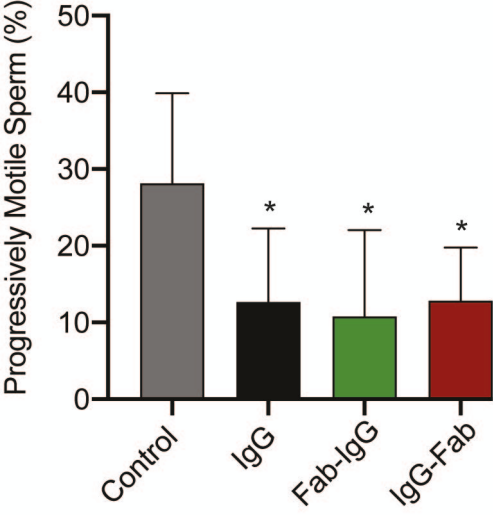


Fab-IgG-1.56 μg/mL



IgG-Fab-1.56 μg/mL





## Supplementary File

### **Engineering tetravalent IgGs with enhanced agglutination potencies for trapping vigorously motile sperm in mucin matrix**

Bhawana Shrestha, Alison Schaefer, Elizabeth C. Chavez, Alexander J. Kopp, Timothy M. Jacobs, Thomas R. Moench, and Samuel K. Lai\*

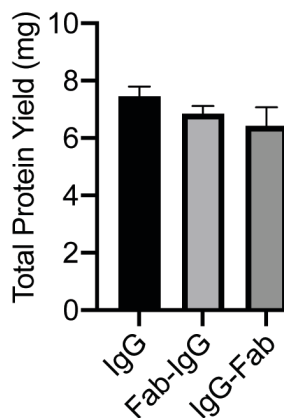


**Fig. S1.** Purified production yield of IgG, Fab-IgG and IgG-Fab from 90 mL Expi293 cells transfection. Data were obtained from 2 independent transfections. Lines indicate arithmetic mean values and standard deviation.

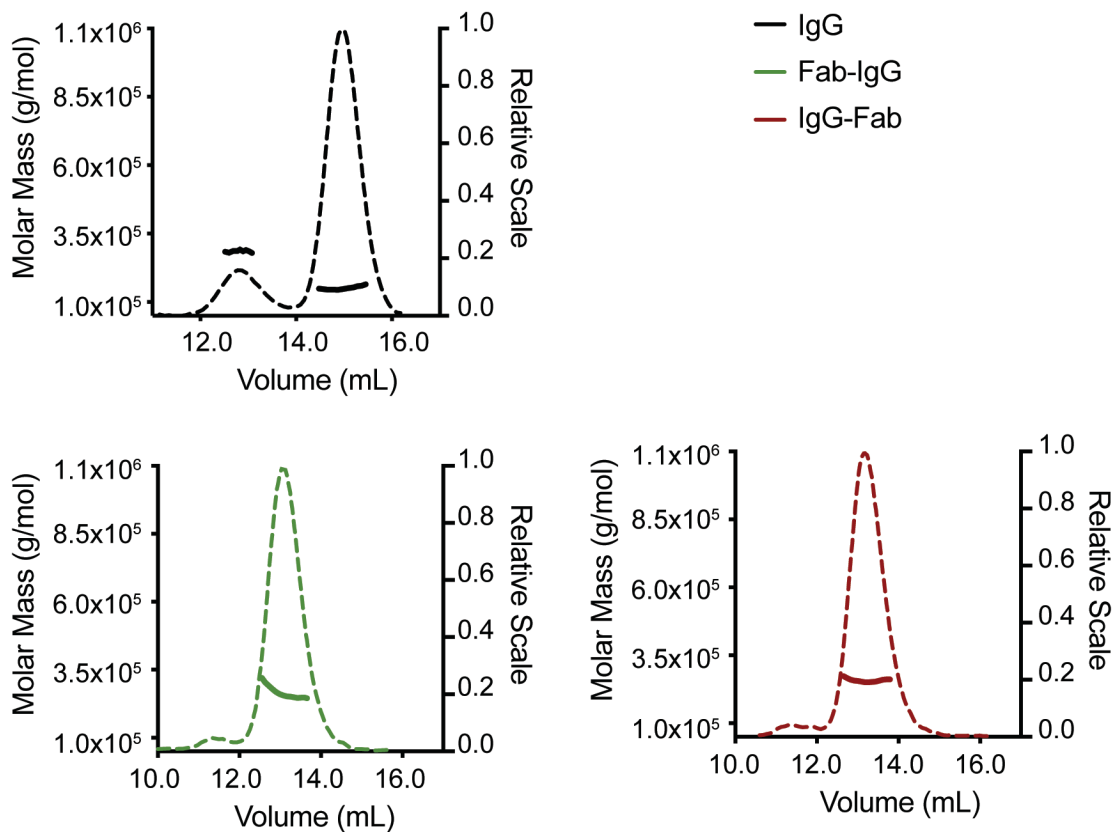


**Fig. S2.** SEC-MALS curves of the indicated Abs. Thick lines indicate the calculated molecular mass (left y-axis) and the dotted lines show the homogenous profile (right y-axis) of the mass for each Ab.

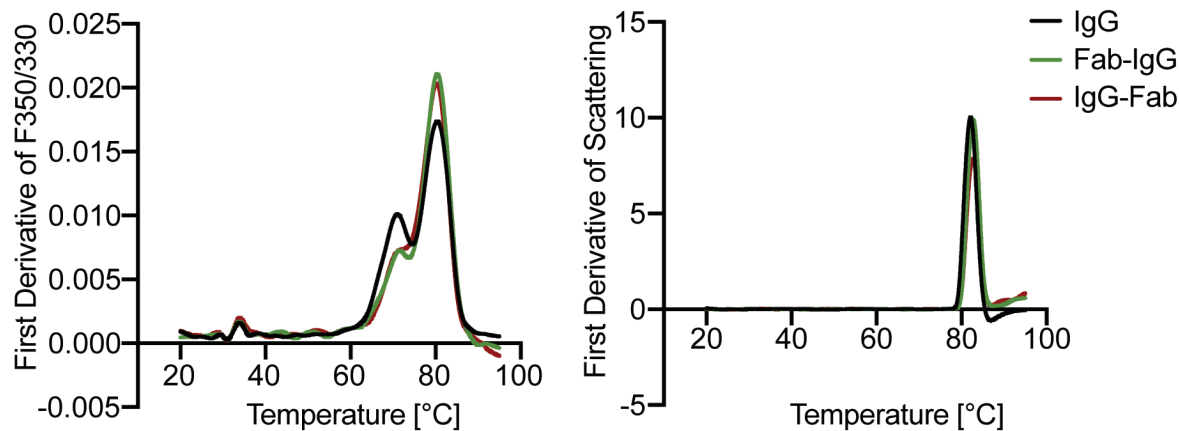


**Fig. S3.** The melting temperatures (left) and aggregating temperature (right) of the indicated Abs as determined by the nanoDSF experiment. The experiment was performed in duplicates and averaged.

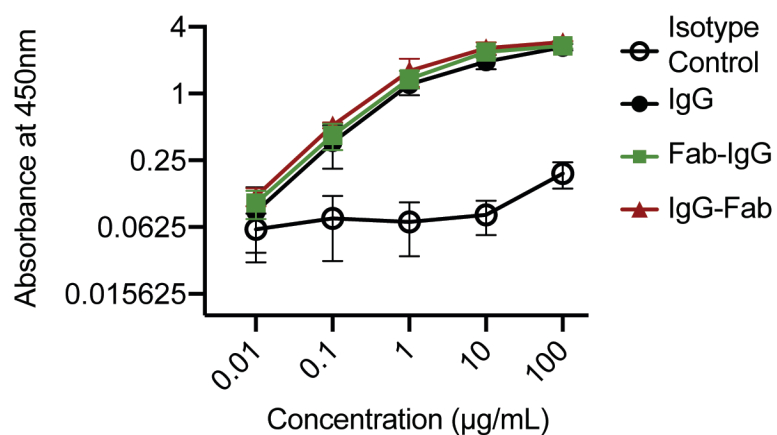


**Fig. S4.** Whole sperm ELISA to assess the binding potency of the indicated Abs to human sperm. Motavizumab (anti-RSV IgG1) was used as the isotype control. Data represent 3 independent experiments with 3 unique semen donors. Each experiment was performed in triplicates and averaged. Lines indicate arithmetic mean values and standard deviation.

**Table S1.** The sperm motility parameters of the Hamilton-Thorne Ceros 12.3.

Parameter	Value	Parameter	Value
Frames Per Sec	60	Path Velocity (VAP)	25 $\mu\text{m/s}$
No. of Frames	60	Straightness (STR)	80 %
Minimum Cell Size	3 pixels	VAP Cutoff	10 $\mu\text{m/s}$
Default Cell Size	6 pixels	VSL Cutoff	0 $\mu\text{m/s}$
Minimum Contrast	80	Slow Cells	Motile
Default Cell Intensity	20	Standard Objective	10X
Chamber Depth	20 $\mu\text{m}$	Magnification	1.87

### Supplemental Movies and Captions

**Movie S1.** Fluorescently labeled motile sperm are not trapped by control IgG 25ug/mL in CVM.

**Movie S2.** Fluorescently labeled motile sperm are trapped by anti-sperm IgG 25ug/mL in CVM.

**Movie S3.** Fluorescently labeled motile sperm are trapped by anti-sperm Fab-IgG 25ug/mL in CVM.

**Movie S4.** Fluorescently labeled motile sperm are trapped by anti-sperm IgG-Fab 25ug/mL in CVM.

